

A butadiyne-linked diruthenium molecular wire self-assembled on a gold electrode surface†

Li-Yi Zhang,^a Hua-Xin Zhang,^b Shen Ye,^b Hui-Min Wen,^a Zhong-Ning Chen,^{*a} Masatoshi Osawa,^b Kohei Uosaki^c and Yoichi Sasaki^{*bc}

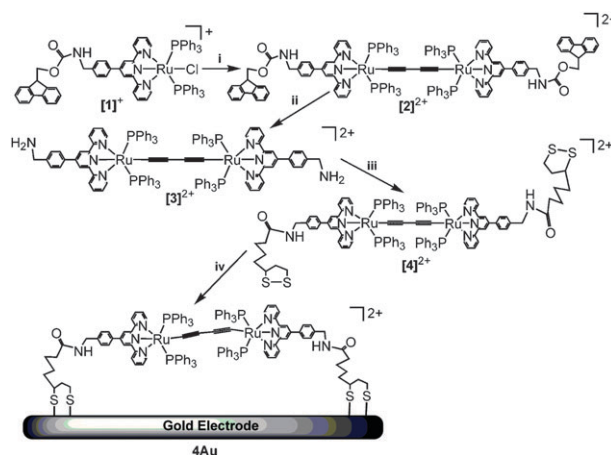
Received 5th August 2010, Accepted 20th October 2010

DOI: 10.1039/c0cc03048a

A 1,3-butadiyne-linked diruthenium complex **4** is successfully brought onto the gold surface in a lying flat mode to form self-assembled monolayers (SAMs) showing reversible multiple redox behaviors on the electrode surface. The diruthenium species with different oxidation states, particularly the Ru₂^{III,III} state which is unstable and impossible to isolate from the solution, can be detected by *in situ* IR spectroscopy.

Linear organometallic complexes with unsaturated carbon chains spanning redox-active metal centers are attractive candidates for molecular wires that facilitate intramolecular electron transfer along the molecular backbone.^{1–3} It is known that self-assembly of functional molecules onto the surface is a key step for their applications in molecular electronics.^{4–7} Inspired by the findings that some thiol-functionalized metal complexes display specific spectroscopic and redox properties upon the formation of self-assembled monolayers (SAMs) onto gold surfaces,^{8–11} we are interested in bringing such organometallic systems onto the solid surface, and examining the intramolecular electron transfer as well as spectroscopic properties. Herein we reported a butadiyne-linked diruthenium system immobilized onto a gold surface in a lying flat mode (Scheme 1) using disulfide-functionalized terpyridine as an ancillary ligand.

As shown in Scheme 1, [2]²⁺ was prepared by reaction of Me₃SiC≡CC≡CSiMe₃ with two equivalents of [1]⁺ *via* fluoride-catalyzed desilylation in a microwave synthesizer at 100 °C for 20 min in *ca.* 30% yield. By oxidation of Ru₂^{II,II} complex [2]²⁺ with [Cp₂Fe](ClO₄) or electrolysis at 0.5 V (*vs.* Ag/AgCl), we were able to isolate a 1-e[−] oxidized complex [2a]³⁺ with a mixed-valence state of Ru₂^{II,III} as a perchlorate salt in 80% yield. Isolation of further oxidized Ru₂^{III,III} species was unattainable. Removal of amino-protecting groups in [2]²⁺ using piperidine gave [3]²⁺ which directly reacted with 5-(1,2-dithiolan-3-yl)pentanoic acid in the presence of *N,N'*-dicyclohexylcarbodiimide, giving the target compound of [4]²⁺ in 50% yield.



Scheme 1 Synthetic routes for [1]⁺–[4]²⁺. (i) Me₃SiC≡CC≡CSiMe₃, KF; (ii) piperidine; (iii) 5-(1,2-dithiolan-3-yl)pentanoic acid and *N,N'*-dicyclohexylcarbodiimide; (iv) self-assembled onto a gold surface.

[2]²⁺ exhibits three redox waves at $E_{1/2} = 0.24, 0.76,$ and 1.34 V in a 0.1 M *n*-Bu₄NPF₆-CH₂Cl₂ solution (see ESI†). These peaks can be ascribed to successive 1-e[−] redox processes of Ru₂^{II,II}/Ru₂^{II,III}, Ru₂^{II,III}/Ru₂^{III,III}, and Ru₂^{III,III}/Ru₂^{III,IV}, respectively.¹² The $\Delta E_{1/2}$ between the subsequent redox waves was approximately 0.52 V. The comproportionation constant K_c for the formation of Ru₂^{III,II} species was 6.18×10^8 , suggesting a quite large Ru··Ru electronic interaction.¹²

The IR spectra of [2](ClO₄)₂ and [2a](ClO₄)₃ isolated gave a C–C stretching mode for the C≡C bond at 1967 and 1855 cm^{−1}, respectively, in the KBr matrix (see ESI†). The UV-Vis spectrum of [2]²⁺ in CH₂Cl₂ displayed an intense absorption in the UV region together with a broad band at 642 nm, arising likely from $d\pi(\text{Ru}) \rightarrow \pi^*(\text{tpy})$ MLCT (metal-to-ligand charge transfer)¹² (see ESI†) transition. Once [2]²⁺ was oxidized to [2a]³⁺, the MLCT band was blue-shifted to 602 nm with a significantly reduced intensity, and two new broad bands appeared at 820 and 1010 nm. The former (820 nm) was probably ascribable to a ligand → Ru^{III} LMCT (ligand-to-metal charge transfer) transition whereas the latter (1010 nm) results most likely from Ru^{II} → Ru^{III} intervalence charge transfer (IVCT) transition.¹² Solvent independence and a high extinction coefficient ($\epsilon = 25\,100 \text{ M}^{-1} \text{ cm}^{-1}$) of the IVCT band together with a large K_c of [2a]³⁺ reveal an electronically delocalized Ru₂^{II,III} system along the molecular backbone. These results indicate that [2]²⁺ and [2a]³⁺ with substituted phenyl terpyridyl ligands preserve the mixed-valence properties similar to their analogs.^{12a}

^a State Key Laboratory of Structural Chemistry, Fujian Institute of Research on the Structure of Matter, Chinese Academy of Sciences, Fuzhou 350002, China. E-mail: czn@fjirsm.ac.cn

^b Catalysis Research Center, Hokkaido University, Sapporo 001-0021, Japan. E-mail: ysasaki@sci.hokudai.ac.jp

^c Division of Chemistry, Graduate School of Science, Hokkaido University, Sapporo 060-0810, Japan

† Electronic supplementary information (ESI) available: Experimental details and figures giving additional spectral and electrochemical properties. See DOI: 10.1039/c0cc03048a

The target compound $[4]^{2+}$ gave two redox peaks at 0.21 and 0.75 V in a 0.1 M $n\text{-Bu}_4\text{NPF}_6\text{-CH}_2\text{Cl}_2$ solution, which can be attributed to the stepwise 1-e^- processes of $\text{Ru}_2^{\text{II,II}}/\text{Ru}_2^{\text{II,III}}$ and $\text{Ru}_2^{\text{II,III}}/\text{Ru}_2^{\text{III,III}}$, respectively (see ESI†), with $\Delta E_{1/2}$ of *ca.* 0.54 V comparable to that of $[2]^{2+}$ (0.52 V). Another quasi-reversible wave that appeared at 1.14 V was ascribable to that of $\text{Ru}_2^{\text{III,III}}/\text{Ru}_2^{\text{III,IV}}$. The negative shift of the redox potentials of $[4]^{2+}$ compared with those of $[2]^{2+}$ indicates the higher electron donation from the alkyl disulfide groups to Ru central ions.

As $[4]^{2+}$ was self-assembled onto a gold electrode surface (denoted as **4Au**), the peak currents of both redox waves are correlated linearly with the scan rates (Fig. 1, inset), indicating that $[4]^{2+}$ is immobilized onto the gold surface. The redox waves due to $\text{Ru}_2^{\text{II,II}}/\text{Ru}_2^{\text{II,III}}$ and $\text{Ru}_2^{\text{II,III}}/\text{Ru}_2^{\text{III,III}}$ processes are observed at 0.25 and 0.88 V, respectively (Fig. 1). The peak separations between the anodic and cathodic peaks are around 50 mV, obviously smaller than those of $[4]^{2+}$ in solution (70–80 mV), indicating an improved redox reversibility of $[4]^{2+}$ after immobilization on the gold surface. The $\Delta E_{1/2}$ (0.63 V) of **4Au** is distinctly larger than that in solution (0.54 V), implying that the SAMs of $[4]^{2+}$ on surface are more favorable for the mixed-valence state of $\text{Ru}_2^{\text{II,III}}$.

The surface coverage of **4Au** estimated from the electric charge of the anodic peak around 0.25 V (Fig. 1) is 1.5×10^{-11} mol cm^{-2} . This value is approximately 43% of the theoretical value (*ca.* 3.5×10^{-11} mol cm^{-2}) assuming that the unit area is $13 \text{ \AA} \times 33 \text{ \AA}$, based on the crystal structure of analogs.¹² Since $[4]^{2+}$ contains four triphenyl phosphine and two phenyl terpyridyl ligands, the head groups of the molecule are very rigid and bulky, it is likely that $[4]^{2+}$ arrays on the gold surface with its two extending tilt arms of alkyl disulfide groups.

To further elucidate the structure and electron distribution of **4Au** on the gold electrode surface, *in situ* surface-enhanced IR absorption spectroscopy (SEIRAS) in the attenuated total reflection mode has been employed during its redox process (see ESI† for detailed experimental conditions for the *in situ* IR measurements).^{9e,f}

Fig. 2a shows a series of *in situ* IR differential spectra (2200–1650 cm^{-1}) simultaneously recorded with a potential sweeping (5 mV s^{-1}) as $+0.50 \text{ V} \rightarrow +1.10 \text{ V} \rightarrow +0.50 \text{ V} \rightarrow 0 \text{ V} \rightarrow +0.50 \text{ V}$, with respect to an IR spectrum obtained at 0.50 V as a reference where **4Au** exists as $\text{Ru}_2^{\text{II,III}}$ (see the arrow in Fig. 1).

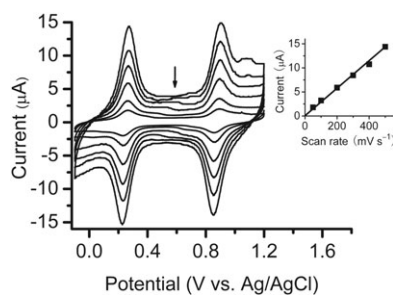


Fig. 1 Cyclic voltammograms (CVs) of **4Au** in a 0.1 M $n\text{-Bu}_4\text{NPF}_6\text{-CH}_2\text{Cl}_2$ solution. The scan rates are 50, 100, 200, 300, 400, and 500 mV s^{-1} , respectively. Inset: a plot of peak current of the anodic wave ($E_{1/2} = 0.25 \text{ V}$) with scan rates.

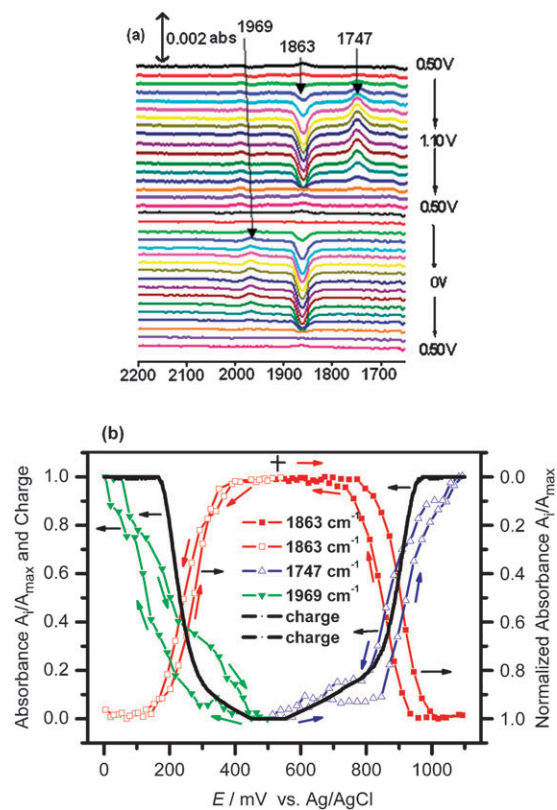


Fig. 2 (a) Time-resolved IR spectra of **4Au** recorded sequentially during a potential sweep from $+0.50 \text{ V} \rightarrow +1.10 \text{ V} \rightarrow +0.50 \text{ V} \rightarrow 0 \text{ V} \rightarrow +0.50 \text{ V}$ at a scan rate of 5 mV s^{-1} in a 0.1 M $n\text{-Bu}_4\text{NPF}_6\text{-CH}_2\text{Cl}_2$ solution. The time resolution is 5 s corresponding to a sampling interval of 25 mV. Each spectrum is co-added from 50 interferograms. The background spectrum was recorded at 0.50 V. (b) Potential dependence of the normalized IR peak intensity (A_i/A_{max}) of three $\nu(\text{C}\equiv\text{C})$ bands and electric charges passed during the potential cycles observed in (a). A_i is the IR peak intensity of $\text{C}\equiv\text{C}$ in each spectrum in (a), and A_{max} is the maximum value.

The upward and downward peaks correspond to the species formed and disappeared, respectively, in comparison with the reference potential.

As shown in Fig. 2a, two IR bands appear at 1863 and 1747 cm^{-1} in the potential cycle between 0.5 and 1.10 V, and two IR bands at 1969 and 1863 cm^{-1} appear in the subsequent potential cycle between 0.5 and 0 V. Fig. 2b shows the IR band intensities (symbols) as well as the electric charge (solid lines) passed as a function of electrode potential. During the cycle in the higher potential region, a downward band at 1863 cm^{-1} and an upward band at 1747 cm^{-1} appear from *ca.* 0.78 V and change quickly with potential and become almost constant when the potential is higher than 0.96 V. In the subsequent negative-going sweeping, these two IR bands change in a reversed way with a small hysteresis to the positive-going sweeping. The potential dependence of the IR band intensities is in agreement with that of charges recorded at each potential during the IR measurement, indicating that the IR bands correspond exactly to the redox process of $\text{Ru}_2^{\text{III,II}}/\text{Ru}_2^{\text{III,III}}$ in the SAM (Fig. 1 and 2b). The pair of IR bands and charges in the potential cycle between 0.5 and 0 V show similar potential behaviors (Fig. 2b) and correlate well with the redox

peaks of $\text{Ru}_2^{\text{II,II}}/\text{Ru}_2^{\text{II,III}}$ in the SAM (Fig. 1). No downward or upward peaks are observed when the potential is swept back to the reference potential (0.50 V), indicating that these redox species are stable and no decomposition takes place in the SAM during the potential cycles.

Based on the comparison with the IR spectra for each isolated diruthenium complex in the KBr matrix and CV results (Fig. 1), IR bands at 1863 and 1969 cm^{-1} can be assigned to $\nu(\text{C}\equiv\text{C})$ of the $\text{Ru}_2^{\text{II,III}}$ and $\text{Ru}_2^{\text{II,II}}$ species, respectively. Although the IR band at 1747 cm^{-1} observed on the surface could not be found in the KBr matrix, this band can be definitely assigned to that of $\nu(\text{C}\equiv\text{C})$ in the $\text{Ru}_2^{\text{III,III}}$ species which is unable to isolate from solution. Therefore, all three oxidation states ($\text{Ru}_2^{\text{II,II}}$, $\text{Ru}_2^{\text{II,III}}$, $\text{Ru}_2^{\text{III,III}}$) of **4Au** have been distinctly identified from the *in situ* IR measurements. As soon as the electron transfer takes place from that of $\text{Ru}_2^{\text{II,III}}$ at 0.50 V, a new peak appeared at 1747 cm^{-1} (1e^- oxidation, $\text{Ru}_2^{\text{III,III}}$) or 1969 cm^{-1} (1e^- reduction, $\text{Ru}_2^{\text{II,II}}$) with the disappearance of itself at 1863 cm^{-1} . As the Ru^{II} central ions are oxidized to Ru^{III} , electrons are expected to flow from $\text{C}\equiv\text{C}$ to Ru^{III} , the bond order of $\text{C}\equiv\text{C}$ is thus reduced and the IR absorption band is shifted to lower frequency (red-shift).¹² Conversely, the reduction process of Ru ion will induce a blue-shift. These results suggest that the oxidation of the Ru ions can significantly affect the electronic state and thus can give useful information for conjugation states of $\text{C}\equiv\text{C}$ with the Ru ions. Firstly, it is interesting to note that the IR band for the $\text{C}\equiv\text{C}$ bond at 0.5 V (corresponding to $\text{Ru}_2^{\text{II,III}}$) gave a single narrow IR band, indicating that the electrons on Ru ions should be definitely delocalized between Ru^{II} and Ru^{III} (i.e. $\text{Ru}^{\text{II.5}}\text{Ru}^{\text{II.5}}$ is a more reasonable notation for the real mixed valence state of $\text{Ru}^{\text{II}}\text{Ru}^{\text{III}}$). Secondly, the peak shifts for $\text{Ru}_2^{\text{II,III}}/\text{Ru}_2^{\text{III,III}}$, $\text{Ru}_2^{\text{II,III}}/\text{Ru}_2^{\text{II,II}}$ are 116 and 106 cm^{-1} , respectively (Fig. 2). In the previous *in situ* IR studies on SAM of the triruthenium cluster $[\text{Ru}_3(\mu_3\text{-O})(\mu\text{-CH}_3\text{COO})_6(\text{CO})(\text{L}_1)(\text{L}_2)]$ ($\text{L}_1 = [(\text{NC}_5\text{H}_4)\text{CH}_2\text{NHC}(\text{O})(\text{CH}_2)_{10}\text{S}]_2$, $\text{L}_2 = 4\text{-methylpyridine}$),^{9a-c} Ye *et al.* reported that the first 1e^- oxidation of the Ru central ions in the SAM induces a large blue-shift for CO ligand (120 cm^{-1}) in comparison with its second 1e^- oxidation (blue-shift, 54 cm^{-1}) and first 1e^- reduction processes (red-shift, 50 cm^{-1}). The large blue-shift in the first 1e^- oxidation step has been successfully explained by the electron localization on the Ru central ions where CO ligand is directly binded. The similar IR peak shifts (116/106 cm^{-1}) and band width (ca. 20 cm^{-1}) for the oxidation and the reduction processes of $\text{Ru}_2^{\text{II,III}}$ in **4Au** SAM indicate similar influence on the $\text{C}\equiv\text{C}$ bonds by the two electron transfer steps from $\text{Ru}_2^{\text{II,III}}$. This confirms that the $\text{Ru}_2^{\text{II,III}}$ state should be a delocalized system from which $\text{Ru}_2^{\text{III,III}}$ and $\text{Ru}_2^{\text{II,II}}$ are formed through 1e^- charge transfer steps with similar band shifts (Fig. 2).

Butadiyne-linked diruthenium complex is successfully immobilized onto a gold surface to form SAMs, in which the Ru-centered redox chemistry is improved and stable mixed-valence state is observed in a better quality. The stability

of the mixed-valence state $\text{Ru}_2^{\text{II,III}}$ is even higher on the surface (K_c is 4.47×10^{10} against 1.34×10^9 in solution). The information on the electronic structures of the SAMs in three oxidation states, particularly the more stabilised mixed-valence $\text{Ru}_2^{\text{II,III}}$ state and the $\text{Ru}_2^{\text{III,III}}$ state which is inaccessible in solution, has been provided by the *in situ* IR absorption spectroscopy.

We thank financial supports from the NSFC (20625101, 20773128, 20821061 and 20931006), the 973 project (2007CB815304) from MSTC, and the NSF of Fujian Province (2008I0027). H.-X. Zhang is grateful to JSPS for a postdoctoral fellowship.

Notes and references

- (a) S. Szafert and J. A. Gladysz, *Chem. Rev.*, 2003, **103**, 4175; (b) R. L. Carroll and C. B. Gorman, *Angew. Chem., Int. Ed.*, 2002, **41**, 4378.
- (a) T. Ren, *Organometallics*, 2005, **24**, 4854; (b) B. Xi and T. Ren, *C. R. Chim.*, 2009, **12**, 321.
- (a) P. Hamon, F. Justaud, O. Cadot, P. Hapiot, S. Rigaut, L. Toupet, L. Ouahab, H. Stueger, J.-R. Hamon and C. Lapinte, *J. Am. Chem. Soc.*, 2008, **130**, 17372; (b) M. A. Fox, R. L. Roberts, T. E. Baines, B. L. Guennic, J.-F. Halet, F. Hartl, D. S. Yufit, D. Albesa-Jove, J. A. K. Howard and P. J. Low, *J. Am. Chem. Soc.*, 2008, **130**, 3566; (c) C. Olivier, K. Costuas, S. Choua, V. Maurel, P. Turek, J.-Y. Saillard, D. Touchard and S. Rigaut, *J. Am. Chem. Soc.*, 2010, **132**, 5638.
- C. Yin, G.-C. Huang, C.-K. Kuo, M.-D. Fu, H.-C. Lu, J.-H. Ke, K.-N. Shih, Y.-L. Huang, G.-H. Lee, C.-Y. Yeh, C.-h. Chen and S.-M. Peng, *J. Am. Chem. Soc.*, 2008, **130**, 10090.
- A. S. Blum, T. Ren, D. A. Parish, S. A. Trammell, M. H. Moore, J. G. Kushmerick, G.-L. Xu, J. R. Deschamps, S. K. Pollack and R. Shashidhar, *J. Am. Chem. Soc.*, 2005, **127**, 10010.
- (a) Z. Ng, K. P. Loh, L. Li, P. Ho, P. Bai and J. H. K. Yip, *ACS Nano*, 2009, **3**, 2103; (b) C. Hortholary, F. Minc, C. Coudret, J. Bonvoisin and J.-P. Launay, *Chem. Commun.*, 2002, 1932.
- (a) T. Kurita, Y. Nishimori, F. Toshimitsu, S. Muratsugu, S. Kume and H. Nishihara, *J. Am. Chem. Soc.*, 2010, **132**, 4524; (b) Y. Nishimori, K. Kanaizuka, M. Murata and H. Nishihara, *Chem.–Asian J.*, 2007, **2**, 367.
- (a) J. Q. Liu, M. N. Paddon-Row and J. J. Gooding, *J. Phys. Chem. B*, 2004, **108**, 8460; (b) N. Madhiri and H. O. Finklea, *Langmuir*, 2006, **22**, 10643.
- (a) S. Ye, W. Zhou, M. Abe, T. Nishida, L. Cui, K. Uosaki, M. Osawa and Y. Sasaki, *J. Am. Chem. Soc.*, 2004, **126**, 7434; (b) Y. Zhang, Y. Tong, M. Abe, K. Uosaki, M. Osawa, Y. Sasaki and S. Ye, *J. Mater. Chem.*, 2009, **19**, 261; (c) W. Zhou, S. Ye, M. Abe, T. Nishida, K. Uosaki, M. Osawa and Y. Sasaki, *Chem.–Eur. J.*, 2005, **11**, 5040; (d) W. Zhou, Y. Zhang, M. Abe, K. Uosaki, M. Osawa, Y. Sasaki and S. Ye, *Langmuir*, 2008, **24**, 8027; (e) M. Osawa, *In situ surface-enhanced infrared spectroscopy of the electrode/solution interface*, in *Advances in Electrochemical Science and Engineering*, ed. R. C. Alkire, D. M. Kolb, J. Lipkowski and P. N. Ross, Wiley, Weinheim, 2006, vol. 9, p. 269; (f) M. Osawa, *Bull. Chem. Soc. Jpn.*, 1997, **70**, 2861.
- M. Abe, T. Masuda, T. Kondo, K. Uosaki and Y. Sasaki, *Angew. Chem., Int. Ed.*, 2005, **44**, 416.
- F. A. Murphy, S. Suárez, E. Figgemeier, E. R. Schofield and S. M. Draper, *Chem.–Eur. J.*, 2009, **15**, 5740.
- (a) L.-B. Gao, S.-H. Liu, L.-Y. Zhang, L.-X. Shi and Z.-N. Chen, *Organometallics*, 2006, **25**, 506; (b) L.-B. Gao, J. Kan, Y. Fan, L.-Y. Zhang, S.-H. Liu and Z.-N. Chen, *Inorg. Chem.*, 2007, **46**, 5651; (c) M. I. Bruce, P. J. Low, K. Costuas, J. F. Halet, S. P. Best and G. A. Heath, *J. Am. Chem. Soc.*, 2000, **122**, 1949.